

May 2020

Numerical Modeling of Magnetic Fields for Mirror Neutron Search Experiment

Adam Johnston

University of Tennessee, Knoxville, ajohn245@vols.utk.edu

Follow this and additional works at: <https://trace.tennessee.edu/pursuit>



Part of the [Electromagnetics and Photonics Commons](#), [Other Mechanical Engineering Commons](#), [Other Physical Sciences and Mathematics Commons](#), and the [Other Physics Commons](#)

Recommended Citation

Johnston, Adam (2020) "Numerical Modeling of Magnetic Fields for Mirror Neutron Search Experiment," *Pursuit - The Journal of Undergraduate Research at The University of Tennessee*: Vol. 10 : Iss. 1 , Article 5.

Available at: <https://trace.tennessee.edu/pursuit/vol10/iss1/5>

This article is brought to you freely and openly by Volunteer, Open-access, Library-hosted Journals (VOL Journals), published in partnership with The University of Tennessee (UT) University Libraries. This article has been accepted for inclusion in Pursuit - The Journal of Undergraduate Research at The University of Tennessee by an authorized editor. For more information, please visit <https://trace.tennessee.edu/pursuit>.

Introduction

The " nn' " Collaboration is a research group involving several universities, including a group of the University of Tennessee, that is performing an experimental search for the neutron to mirror neutron transformation at Oak Ridge National Laboratory in the High Flux Isotope Reactor [1]. Theoretical models suggest [3, 4] that neutron can be transformed into mirror neutron, which is a sterile particle for ordinary matter (OM). Mirror neutrons, if they exist, can be part of the Mirror Matter (MM) particles that can constitute the Dark Matter (DM) in the universe. Theory also suggests that MM is simply a copy of the Standard Model with exactly the same particle content and forces, but not interacting with OM except through gravity [3,4]. Besides that, there might exist a new force that would transform neutron (n) to mirror neutron (n') [3, 4]. The search for such a force and the transformation or oscillation $n \rightarrow n'$ is the purpose of the HFIR experiment.

Since neutrons have a magnetic moment, the magnetic field will change the OM neutron's potential energy. The potential energy of mirror neutron will not be affected by an OM magnetic field, but the possible presence of MM field on Earth with unknown magnitude would affect the potential energy of mirror neutron, therefore affecting the energy gap between the two states. Thus, the oscillation of $n \rightarrow n'$, when separated by large energy gap, will be heavily suppressed until the OM magnetic field will compensate MM magnetic field in magnitude and direction such that two energy levels will become equal. In the experiment at HFIR it is planned that a magnetic field will be changed step-by-step in a controlled way and will be uniform. The magnitude of the mirror magnetic field is assumed to be uniform on the scale of experiment, but unknown (magnitude and direction cannot be directly measured). In the experiment, the OM magnetic field will be varied in magnitude and direction within ± 0.5 G range and should remain uniform within ± 2.5 mG. Thus, a scan of the magnetic field should reveal the resonance in the probability of $n \rightarrow n'$ and in inverse probability $n' \rightarrow n$, as described in Ref. [1]. The goal of this work is to model the realistic configuration of a three-dimensional (3D) magnetic field produced by 3D coils of conductors with the constant controlled current around a large volume of vacuum chamber in experiment [1]. The length of the stainless steel vacuum chamber is 20 m and diameter 2.5 m. Uniformity ± 2.5 mG should exist along the axis of the chamber in a volume with radius of ~ 6 cm.

Methodology

The calculations in the model use numerical integration over small elements to approximate continuous wires. Bio-Savarts Law is used to describe the integrated magnetic field, B , from a current carrying wire element, $I\vec{dl}$.

$$\vec{B} = \int \frac{\mu_0(I\vec{dl} \times \vec{r})}{4\pi|r|^3} \quad (1)$$

Although the experiment will use OM magnetic field in varying 3D directions within magnitudes ± 0.5 G, the model was set to create a $\vec{0}$ field as a result of compensation of external uniform Earth magnetic field, to get a clear picture of the characteristics of the field. The values used for Earth's magnetic field were gathered from the National Center for Environmental Information [2]. Due to the fact that vector fields (such as magnetic fields) add linearly, similar uniformity will be maintained for all magnitudes and directions of field created in the apparatus. As the Bio-Savart Law calculates the field at a point, the volume of interest within the vacuum tube was represented by a 3D mesh-grid with the z axis running the length of the tube, the axis x running horizontally, and the axis y running vertically forming right-hand coordinate system, as shown in Fig. 1. Calculations were taken every square centimeter in the xy-plane and xy-planes were measured every .25 meter in the z-direction. Calculations were taken in this manner because the gradient of field is much higher in the xy-plane as compared to the z-direction. The field is created by two sets of Helmholtz coils running the length of the tube, which control the field in the xy-plane, and by a large solenoid, which controls the field in the z direction (Figure 1). It should be noted that while the field created by a typical solenoid is perfectly uniform within the loops, this apparatus does not create that effect since there is considerable space between the solenoid loops. Creating a solenoid with no space between the loops would be infeasible due to the amount of wire required. Each point on the grid contains the sum of field in projections on axes which are calculated from each of the straight sections of Helmholtz coils, running the length of the tube, as well as from the solenoid surrounding the tube, and a set of straight connecting wires representing the Helmholtz coils at the ends of the tube.

To ensure the field is as uniform as possible along the z axis the wires will be looped perpendicular to the running length of the tube, then the wire will be brought to the next loop as shown in Figure 1. Returning the wire along the line it was brought out on will negate the excess magnetic field from wire between each loop.

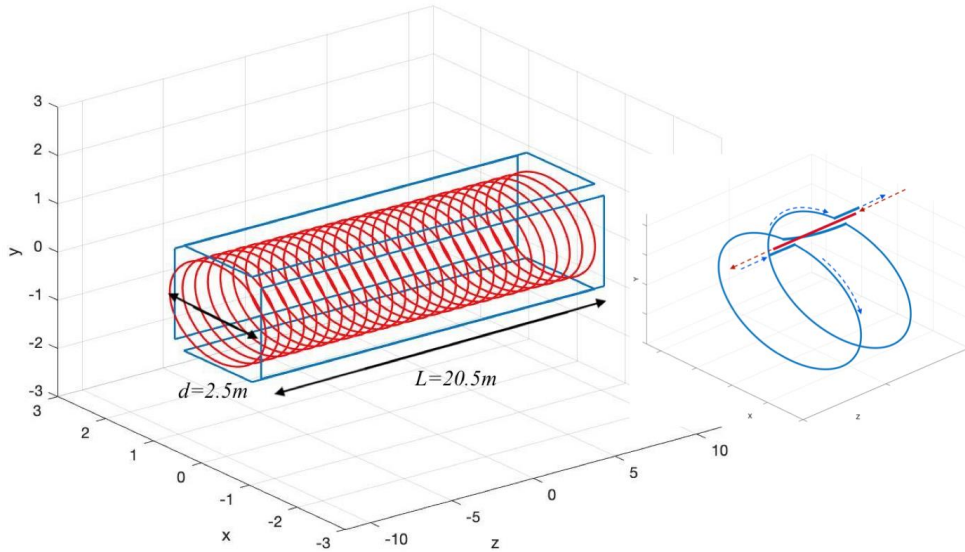


Figure 1: Dimensions and current direction of the wire apparatus. The diagram on the right outlines the placement of wires in the solenoid apparatus, since the outgoing and returning wires are close and running parallel their fields negate each other. In the left diagram the red lines represent the solenoid's wire placement, and the blue lines represent the Helmholtz coils.

| Wire Placement (m) | |
|-----------------------------------|-------------|
| Y-field Coils (x,y) | (0.71,1.09) |
| X-field Coils (x,y) | (0.9,0.94) |
| Solenoid radius | 1.25 |
| Solenoid Spacing (n=27 loops) | 0.775 |
| Solenoid starting point (z_0) | -10.25 |

Table 1: The Helmholtz coils are placed symmetrically about the origin, the coordinates of the wire through quadrant one is given.

To create the magnetic field model, each current component was described by an infinitely thin line in three-dimensional space, that line was numerically integrated over, with a dl of 1 cm. The thickness of the wires will not impose any significant error as they are negligible when compared to the scale of the model. To simplify the calculations, the wires were segmented into simple

shapes; the two Helmholtz coils were broken up into eight straight segments running the length of the beam line with eight narrow ellipses representing the ends of the coils. The error introduced by using simple shapes will be negligible; while the apparatus will not perfectly resemble the model in construction, it will be built as precisely as possible. The error from these approximations is expected to be on the scale of magnetic field fluctuations due to other experiments in the laboratory. To justify this claim I will estimate the error from a ‘worst case scenario’ which is that the experiment uses a single large wire (as opposed to several smaller wires) to create the Helmholtz apparatus. This large wire would be 3/0 AWG if it were copper, which is rated for ~210 Amps and it has a minimum bending radius of ~10 cm . Using this bending radius we can calculate the difference in wire length between a rectangular Helmholtz apparatus and one with rounded edges, which comes out to be ~.17m or ~.4% error in wire length. Using Ampere’s Law, Equation 2 where integral is carried out over a closed curve of wire, we can see that this leads to a ~.4% change in field magnitude. (2)

$$\oint_C \vec{B} \cdot d\vec{l} = \mu_0 I$$

The solenoid was represented by successive circles running the length of the tube, and starting at a z_0 value spaced by .775m. The length of the wire apparatus is constrained by other components of the experiment placed at the end of the tube such as particle detectors. The value of current for the Helmholtz coils and solenoid loops were estimated by Equations 3 and 4. The current in each Helmholtz coil set was calculated using Equation 3, such that $(x_u, y_u, z_u) = (0,0,3.33)$. To understand the reasoning for this you must realize that the field in the beam tube is greatly affected by end effects. This means that at most only two points of $\vec{0}$ field can be created (since the problem is symmetric). By moving these $\vec{0}$ points apart and keeping track of average field magnitude, it was found that placing these points at $(x_u, y_u, z_u) = (0,0,3.33)$ & $(0,0,-3.33)$ gave the lowest average field magnitude and therefore the lowest variance. Two identical equations regulate the current for the Helmholtz coils were used due to the fact that Earth’s field is not equal in the x and y directions, so the same calculation is carried out for I_x and I_y however $|B|$ changes. Figure 2 contains an explanation for the notation in Equation 3. Equation 4 calculates the strength of field created by the whole of the solenoid array. z_0 represents the starting z value of the N sized solenoid grouping, each solenoid is spaced by the value l_i . r represents the radius of the solenoid loops.

$$I_x = \frac{|B|\pi R}{\mu_0(\sin(\theta_a) + \sin(\theta_b)\cos(\phi))} \quad (3)$$

$$I_{solenoid} = \frac{B_z \sum_{i=0}^N (z_0 + l_i)^2 + r^2)^{\frac{3}{2}}}{\mu_0 r^2} \quad (4)$$

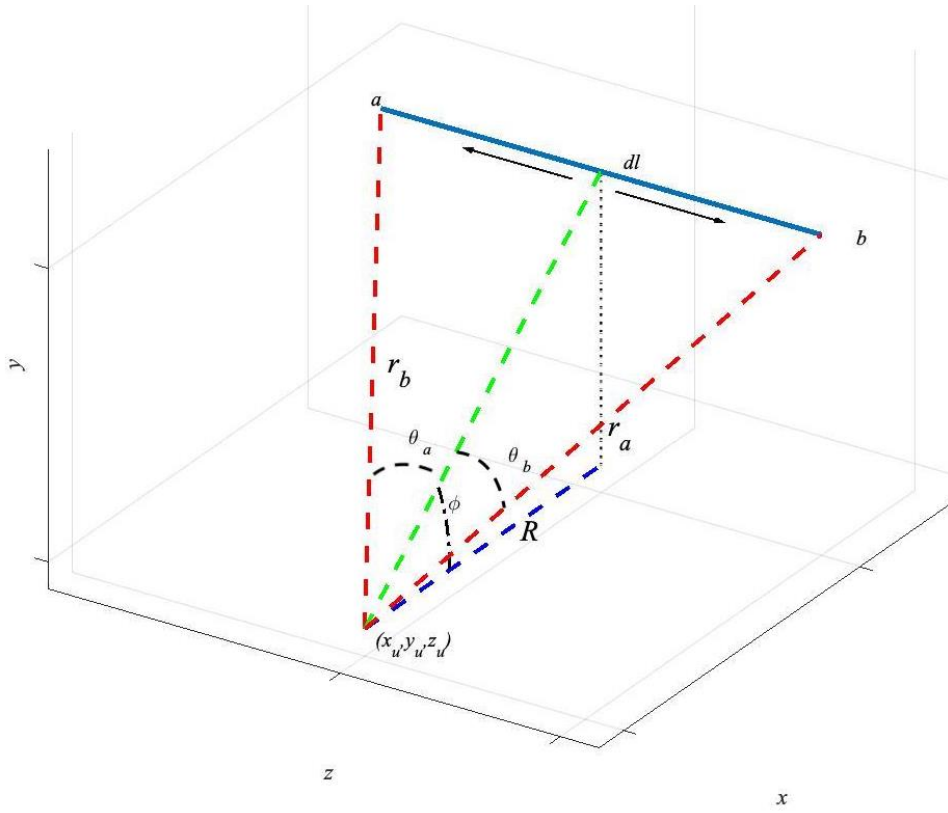


Figure 2: Legend for Equation 2 , about some point u .

Using the given current values, the field vector at each grid point is calculated by creating a dx_t , dy_t and dz_t array containing the position of a the current element in each axis, where t is a place-keeping index. This effectively maps each $dl \rightarrow$ on the element $dx_t dy_t dz_t$ (from Eq. 1). For the straight sections of the Helmholtz coils dz_t contains a list of indices in 1 cm increments (each index representing a section Idl of wire) to span the beam line, dx_t and dy_t are $\vec{0}$ vectors in this case. Concerning the solenoid, dx_t and dy_t are written as $r(\cos(\phi_t) - \cos(\phi_{t-1}))$ and $r(\sin(\phi_t) - \sin(\phi_{t-1}))$ respectively, where ϕ is the angle rotating clockwise around the z axis (equivalent to ϕ in Eq. 3). Values ax_t , ay_t and az_t represent the distance from a point of calculation to each current element, dl . Every point of calculation has its own set of ax_t , ay_t and az_t . Once these values are created, the cross product is calculated between the point of calculation and each current segment by grouping the variables as if they were entries of a vector in \mathbb{R}^3 , they become $[dx_t, dy_t, dz_t]$ and $[ax_t, ay_t, az_t]$, where $[dx_t, dy_t, dz_t] \equiv dl$ and $[ax_t, ay_t, az_t] \equiv r$. However, each entry is essentially a $1 \times n$ array so the multiplication in the cross product must be conducted element wise. The result is three new vectors representing the components of the cross product which can be substituted into Equation 1 in place of $(dl \times r)$. Current, I , is pulled out of the cross

product and multiplied along with the rest of the variables, the equation is summed in order to numerically integrate along dl . The final values of field strength are stored in a B_x , B_y , and B_z arrays, which once each point has been calculated are size $[N, M, P]$ where N defines the x-axis, M defines the y-axis, and P defines the measurements along the z-axis (again, calculations are taken every cm in xy-plane, and xy planes are calculated every .25 m). For the data shown here $[N,M,P]=[51,51,81]$.

Discussion

As the goal of the experiment is to scan the magnetic field between ± 1 Gauss (for any chosen direction of field C) while maintaining field uniformity at the level ± 2.5 mG in the maximum volume, preset field equations were added to the calculations matching Equations 3 and 4 with, B_x and B_z replaced with the desired field strength. When the experiment is run, these equations can be used to create a list of current values for scanning field directions.

| Field Uniformity (Gauss) | | | |
|--|--------|-------------------------|--------------------------|
| Total calculated volume (.5 × .5 × 20m) | | (r=.0575m, full 20m) | (r=.0575, middle 16m) |
| σ (x-comp) | 0.0314 | 0.001228 | 0.000394 |
| σ (y-comp) | 0.0406 | 0.001589 | 0.000510 |
| σ (z-comp) | 0.0246 | 0.000961 | 0.000302 |
| $ \sigma $ | 0.0569 | 0.002226 | 0.000712 |

Table 2: The values in the right most two columns are calculated from within the specified radius. The values in the left-hand side represent the whole area of interest.

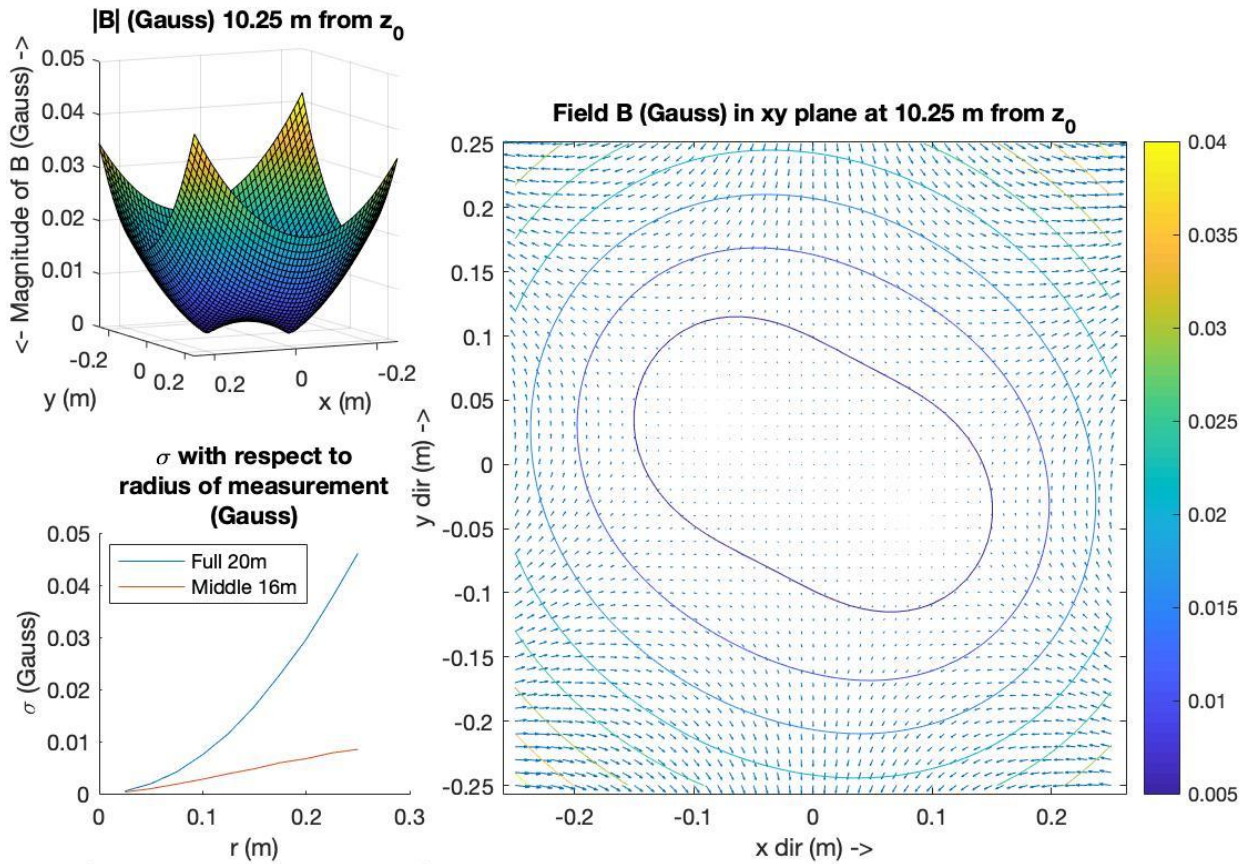


Figure 3: Field Strength on a plane at the center of the tube is shown on the right. As we move towards the center of the tube along the z axis, the field behaves more like it was under the influence of an infinite wire, therefore becoming more and more uniform.

Information on the field's distribution is given in Table 2, the values were calculated over the entire grid within several volumes. As you can see, the field uniformity meets the goal of $\sigma = 2.5 \text{ mG}$ for a small portion of the total volume, and as the aperture of the area of interest decreases so do the standard distribution values, this is because of the $\frac{1}{r^2}$ dependence of Bio-Savart's Law. The double peaks of the field in the Figure 3 are due to the fact that the coils are positioned in such a way that their fields are pointing in congruent directions along one diagonal and opposing directions along the other diagonal. As the distance from the plane at which the field is calibrated increases, the minimums move out radially, in the plane which the field is calibrated the two minimums meet in the middle to form a singular peak.

This method of numerical integration serves as a useful approximation for calculating magnetic fields from complex shapes as it only requires a function of the wire segments' position to be parametrized then summed over as opposed to analytically carrying out an integral. Another solution which avoids the problem of integrating a potentially complex function could be to use a preloaded numeric integration function. This is a perfectly valid method, however, in this case is

uses an unnecessary amount of precision which will slow run time. A slow run time can be mitigated by minimizing the number of calculation points, however in many cases a fine view of field behavior is necessary and there is no avoiding creating a computationally intensive program. The results discussed in this paper have been validated by comparison to an analytically computed Bio-savart integral. The field from one meter away from the center of a straight 15m, 10 Amp current segment was calculated using both methods. The numeric method creates a 0.66% error when compared to the exact integral. The numeric approximation used 1cm dl length as in the model.

| Technical Data | |
|---------------------|---------------------|
| Wire Group | Total Current (Amp) |
| Helmholtz Coils (x) | 193 |
| Helmholtz Coils (y) | 101 |
| Solenoids | 18.4 |

Table 3: The Table current required to create a 0^{th} field, these values will be changed by up to a factor of ~ 2 when scanning field magnitudes.

As shown in Table 3, the apparatus, especially the Helmholtz coils, require a significant amount of current. The Helmholtz coils both use $\sim 170\text{m}$ of wire, and the solenoid grouping uses $\sim 212\text{m}$ of wire, if a single wire is used. Creating enough current for a single wire set up, however, will not be feasible. If The experiment will use 20 Amp current sources, therefore multiple insulated wires stranded together will have to be used to create an equivalent field to a single wire carrying a large current. Since the experiment must scan field strengths of $\pm 0.5\text{G}$ the apparatus will need to be capable nearly doubling its field strength. Therefore, we will use 19 wires to create field in the x-direction and 11 wires for field in the y-direction, the solenoid loops will use 2 wires. Accounting for this the total cost of wires will come to approximately \$2000. Helmholtz wires will be held in place by a specially designed supports attached from outside to the vacuum tube, and the solenoid will simply be coiled around the beam tube and secured with adhesive and wire guides.

Conclusion

We demonstrated that the goal of uniformity $\pm 2.5\text{ mG}$ in the whole field range $\pm 0.5\text{ G}$ in the large 3D coil can be achieved. It should be noted that when measured alone the middle 16m of the tube has a much better uniformity than the total length. This suggests that the goal of $\pm 2.5\text{ mG}$ uniformity for the 20m tube could be significantly improved upon with the wire apparatus were lengthened. Moreover, the model provides the sufficient calculations to predict the placement and current of wire to create the necessary fields for the magnitude and direction scanning required for the proposed experiment. The next steps of the development will be to create a scale model of the beam tube then run a scaled numerical modeling experiment, and measure the field with a magnetometer. Once the computer model has been validated, the full scale model can be designed to put to use in the experiment to search for mirror matter.

References

- [1] L. J. Broussard, K. M. Bailey, W. B. Bailey, J. L. Barrow, B. Chance, C. Crawford, L. Crow, L. Deeber-Schmitt, N. Fomin, M. Frost, A. Galindo-Uribarri, F. X. Gallmeier, L. Heilbronn, E. B. Iverson, Y Kamyshkov, C.-Y. Lui, I. Novikov, S. I. Penttil^a, A. Ruggles, B. Rybolt, M. Snow, L. Townsend, L. J. Variano, S. Vavra, A. R. Young. *The New Search for Mirror Neutrons at HIFR*. arXiv:1710:00767v2 [hep-ex] 25 Oct 2017.
- [2] National Oceanic and Atmospheric Administration: National Center for Environmental Information. *Magnetic Field Estimated Values*. 2015.
<https://www.ngdc.noaa.gov/geomag/calculators/magcalc.shtml#igrfwmm>
- [3] Z. Berezhiani and L. Bento, Phys. Rev. Lett. **96**, 081801 (2006)
doi:10.1103/PhysRevLett.96.081801.
- [4] Z. Berezhiani, Eur. Phys. J. C **64**, 421 (2009) doi:10.1140/epjc/s10052-009-1165-1.